Journal of Magnetic Resonance 198 (2009) 222–227

Contents lists available at ScienceDirect

Journal of Magnetic Resonance

journal homepage: www.elsevier.com/locate/jmr

Design of a permanent magnet with a mechanical sweep suitable for variable-temperature continuous-wave and pulsed EPR spectroscopy

C. Bauer, H. Raich, G. Jeschke [1], P. Blümler *

Max Planck Institute for Polymer Research, Postfach 3148, 55021 Mainz, Germany

ARTICLE INFO

Article history:
Received 26 September 2008
Revised 13 February 2009
Available online 27 February 2009

Keywords:
ESR
Electron spin resonance
Electron paramagnetic resonance
Copper
ESEEM
ENDOR
Nested Halbach dipoles

ABSTRACT

A magnetic system is introduced which consists of three nested rings of permanent magnets of a Halbach dipolar layout and is capable for EPR spectroscopy. Two of the rings can be rotated independently to adjust the magnetic flux in the center and even allow for mechanical field sweeps. The presented prototype achieves a magnetic flux range of 0.0282–0.3013 T with a minimal sweep of 0.15 mT and homogeneity of about 10^{-3}.

First applications with CW and pulsed Mims ENDOR as well as ESEEM experiments on a sample of a glycine single crystal doped with 1% copper nitrate demonstrate that flux range, sweep accuracy and homogeneity of this prototype is sufficient for EPR experiments on most solid samples.

Together with a recently improved design magnets can be build which could serve as compact and easily transportable replacement of standard electromagnets with negligible consumption of power or coolants.

1. Introduction

Since the advent of commercial spectrometers at the end of the 1980s pulsed electron paramagnetic resonance (EPR) spectroscopy [1] has spread from a small community of method developing groups to a significant fraction of the groups that are mainly concerned with EPR applications in physics, chemistry, and biology. The recent surge of distance measurements in the nanometer range by pulsed EPR [2,3] on spin-labeled biomacromolecules [4,5] indicates a great potential for further widening of the application of pulsed EPR in structural biology. Continuous-wave (CW) EPR spectrometers at X-band frequencies of about 9.6 GHz can be built with small electromagnets that may not even need water cooling or with permanent magnets [6–13]. However, the existing designs are not well suited for a pulsed EPR spectrometer. First, the gap of the magnet is too small to accommodate a pulsed EPR probehead inside a cryostat, as is necessary since most pulsed EPR experiments have to be performed with liquid nitrogen or liquid helium cooling. Second, while the major contribution to the magnetic field is supplied by the permanent magnet, adjustment of the electron spin resonance frequency to the fixed microwave frequency of the spectrometer is achieved by an additional sweep coil which continuously consumes electrical power. This is not a disadvantage for CW EPR experiments where the field is swept during the whole measurement process, but causes unnecessary power consumption in the majority of pulsed EPR experiments that are performed at fixed field and frequency. Additionally, such coils require extra space and generate heat, which might change the temperature of the permanent magnets and hence the resulting field. On the other hand, sweep capability for the magnetic field is required to record the EPR spectrum of the sample before setup of the pulse experiment and to adjust the resonance field to the desired position in the spectrum.

Here we present the design of a permanent magnet with a resulting magnetic field which can be mechanically swept and can be operated at a fixed field without power consumption at any point within its sweep range. Furthermore, it is big enough to accommodate a standard flow cryostat and probe head as used in current commercial X-band pulse EPR spectrometers. The complete magnet consists of three nested Halbach Mandhala magnet rings that can be rotated with respect to each other by two stepper motors and has a flux range from 0.0282 to 0.3013 T. The field homogeneity is sufficient for EPR applications as is demonstrated by CW EPR, electron spin echo envelope modulation (ESEEM) and pulsed electron nuclear double resonance (ENDOR) experiments on Cu(II) doped into a crystal of glycine. The magnet has a size of 840 × 440 × 340 mm and weighs 47 kg. The size for instrumentation (probeheads and cryostats) is limited by the inner diameter of 80 mm.

Recently this design has been improved to generate 0.2–0.45 T with a homogeneity of better than 400 Hz (i.e. ca. 50–20 ppm) over

* Corresponding author. Address: Forschungszentrum Jülich GmbH, Institut für Chemie und Dynamik der Geosphäre, ICG-3: Phytosphäre, Geb. 06.2 (E5), 52425 Jülich, Germany. Fax: +49 2461 61 2492.
E-mail address: p.bluemler@fz-juelich.de (P. Blümler).
[1] Present address: ETH Zürich, HCI F227, 8093 Zürich, Switzerland.

1090-7807/$ - see front matter © 2009 Elsevier Inc. All rights reserved.
doi:10.1016/j.jmr.2009.02.010

5 mm DSV (diameter of a spherical volume). This magnet consists only of two nested Halbach rings and weights about 30 kg. However, it was not equipped with a mechanical sweep [14].

2. Materials and methods

2.1. Sample preparation

A concentrated solution of glycine (Aldrich) in deionized Milli-Q water was doped with 1 Mol% copper(II)nitrate (Aldrich). Slow evaporation of the water at ambient temperature provided pale blue crystals of a convenient size for measurements in a standard EPR tube (Wilmad).

2.2. EPR measurements

All EPR measurements were performed with a Bruker Elexsys 580 spectrometer at a temperature of 15 K, using helium cooling with a flow cryostat (Oxford instruments). The whole flow cryostat (outer diameter of 70 mm), which doubles as a probe holder in the Bruker spectrometer, was placed inside the bore of the home-built magnet. Because the field generated by permanent magnets is temperature dependent (here a drift of about a tenth of a sweep step was observed over temperature drifts of about 3 °C, see also Table 1), the measurements were conducted in an air-conditioned lab at $T = 23 \pm 0.5$ °C (measured over a duration of 10 h). The probehead was connected to the microwave bridge of the spectrometer by a flexible coaxial microwave cable of 1.5 m length. CW EPR at a frequency of 9.768105 GHz was performed with a power of 20 μW (40 dB attenuation) and a modulation amplitude of 0.2 mT. The sweep acquisition of the spectrometer was externally triggered by a TTL signal derived from a contact switch at the magnet. The actual sweep width of 10 mT was set by adjusting the sweep times of the home-built magnet and of the spectrometer. No further synchronization during the sweep was applied. The CW EPR spectrum is the sum of ten scans.

Mims ENDOR was performed with a repetition time of 1.024 ms and pulse lengths of 28 ns for the microwave π/2 pulses and 14 μs for the radiofrequency pulse. A [(+x)−(−x)] phase cycle was performed on the first π/2 pulse to obtain zero baseline. The spectrum is the sum of 9 scans with two times 100 shots per scan corresponding to a total measurement time of 60 min. Three-pulse ESEEM was performed with a repetition time of 2.048 ms and pulse lengths of 28 ns for the π/2 pulses and a [(+x,+x)−(−x,+x)−(+x,−x)+(−x,−x)] phase cycle on the first and last pulse to cancel echo crossings. The delay between the first two pulses (rising flank to rising flank) was 200 ns and the initial delay between the second and third pulse was 320 ns. The time trace consists of 2048 data points with an increment of 16 ns. The time trace is the sum of 5 scans with four times 30 shots per scan corresponding to a total measurement time of 42 min.

Table 1
Summary of the technical data.

Physical dimensions	Number	Length (mm)	Width (mm)	Height (mm)
Magnet system	1	800	400	500
Magnet blocks	576	13	13	17
Weight/Diameterss		**Weight (kg)**		**Inner bore (mm)**
Magnet		75		81
Controller		15		
Field range		**Minimum**	**Maximum**	**Min. step**
Magnet [G]		282	3014	1.5
Temperature drift [G/K]			−0.05	
Homogeneity		See Fig. 3		

3. Results and discussion

3.1. Concept of the permanent magnet

Two-dimensional magnetization patterns possessing one-sided flux were first proposed theoretically in 1973 by Mallinson [15]. These were referred at the time as a "magnetic curiosity", and later realized by Klaus Halbach [16,17], who developed this idea further, and constructed arrangements of permanent multipole magnets, nowadays known as Halbach arrays. They can consist of a different number of individually shaped magnets, depending on the particular layout and purpose of the magnet-arrangement. The optimized construction of dipolar, circular Halbach arrays from identical magnets was described by Raich and Blümler [13]. The advantage of using identical rather than individually shaped and magnetized magnets is explained by the strong variation (up to 10%) of the magnetic properties of commercially available materials. In order to construct Halbach arrays with homogeneities better than 10^{-3} the magnets can be arranged in such ways that their deviations compensate- a process which is easier realized with a large number of "identical" magnets. The magnetic field inside the resulting arrays is perpendicular to the principal axis of the cylinder, having mainly planar components. Ideally the magnetic field is completely confined inside the cylinder, hence, making optimal use of the mounted magnetization and achieving high homogeneities (typically $\Delta B/B < 10^{-3}$).

3.2. Magnet design

The properties described above allow for characterizing the resulting magnetic flux inside a Halbach circular dipole array by a single vector. Consequently such circular arrays can be concentrically nested one inside the other with the possibility to perform mechanical rotations with only small torque relative to each other by angular displacement θ [18]. As a result the total magnetic field at its center varies as a function of this angle [14,18–20]. When non-linearities in the magnetic hysteresis loop can be ignored (as it is the case with the magnetically very hard rare-earth alloys), the total magnetic field is the vectorial sum of the magnetic fields from all nested arrays. If two Halbach circular arrays are designed in such a way that their magnetic fluxes have the same magnitude B, it is in principle possible to vary the total magnetic flux from zero, when the vectors are antiparallel ($\theta = 180°$), up to $2B$ for parallel flux vectors ($\theta = 0°$). In reality however, imperfections in construction, dimensional tolerances and homogeneity of the permanent magnets limit these ideal values.

The objective of this work was to devise a magnet arrangement which allows a coarse adjustment of the magnetic field to the desired EPR resonance by two rings while a third ring with a weaker field allows a mechanical field sweep around this value.

The inner ring is fixed and its flux vector (B_i) defines the z-direction. The middle ring and hence its flux vector (B_m) is rotated relative to z by an angle θ while the outer ring (B_o) is at an angle φ relative to z. The resulting magnetic flux, B_e, is then the vector sum of all three vectors and amounts to

$$B_e = \sqrt{B_i^2 + B_m^2 + B_o^2 + 2B_i(B_m\cos\theta + B_o\cos\varphi) + 2B_mB_o(\sin\theta\sin\varphi + \cos\theta\cos\varphi)} \quad (1)$$

Following the concept of NMR-Mandhalas [13] all three rings were designed to be assembled from identical magnet blocks (dimensions 17 × 17 × 14 mm) of FeNdB (maximum energy product about 45 MGOe and a remanence of $B_r \approx 1.35$ T, produced by Ningbo, Ningang, Peoples Republic of China). This design (see Fig. 1) results in the following values: the inner ring with 16 magnets provides 48% of the total maximal field or $B_i = 145$ mT, the middle ring 30%

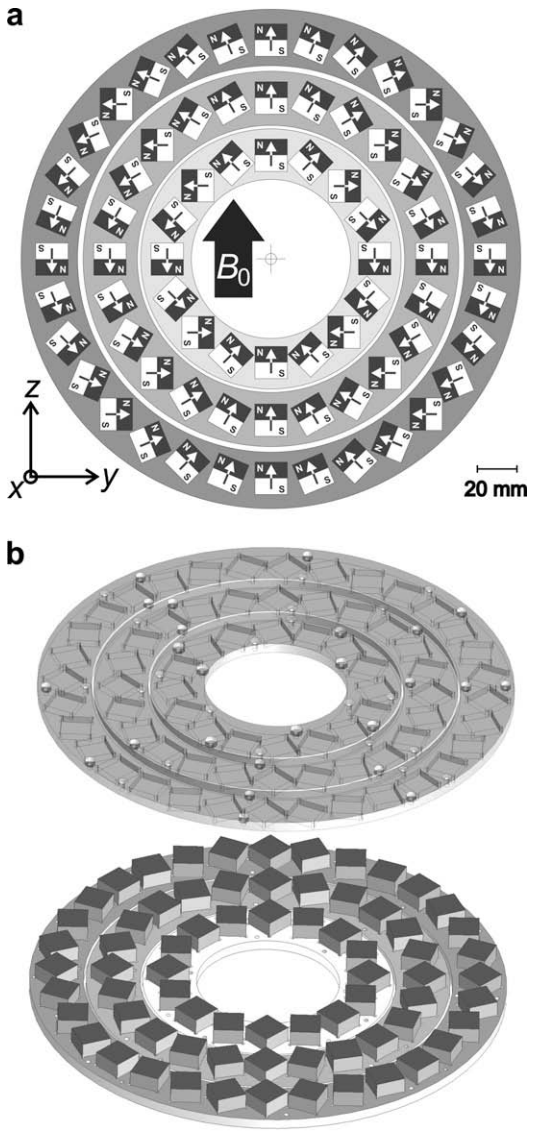

Fig. 1. Schematic design of the Halbach permanent magnet: (a) positioning of the identical magnet blocks in the three nested rings. Note the coordinate system for the nomenclature used in this publication. (b) Assembly of a single layer of the magnet assembly. See text for more details.

or B_m = 90 mT and the outer ring 22% or B_o = 65 mT. Each layer was mounted in an aluminum support with milled sockets to house the magnets (see Fig. 1b). These layers are then stacked using threaded rods and fixed by nuts (see Fig. 2a). Free rotation of the middle and outer stack is assured by ball-bearings at their lower ends (see Fig. 2b). The rotation angles are adjusted via two toothed belts driven by stepper motors (Systro, Germany) controlled by home-built electronics which is interfaced to the EPR spectrometer (see Fig. 2b–d). The technical data of the magnet system are summarized in Table 1.

3.3. Magnet performance

3.3.1. Flux range and resolution

The magnet was constructed as part of a home-built S-band pulsed EPR spectrometer operating at a typical frequency of 3.5 GHz. This frequency corresponds to $h\nu/\mu_B$ = 0.25 T so that a g value range from g = 1 to g = 8 can be covered with a sweep range from 0.03 to 0.25 T. The actual flux range measured by a Hall probe extends from 0.0282 to 0.3013 T if the two outer magnet rings are rotated. If only the middle ring is rotated and the outer ring is fixed in an orientation where its flux adds to the flux of the inner ring, the range extends from 0.1277 to 0.3004 T, corresponding to a sweep range of 0.1727 T. Rotation of the outer ring only provides a sweep range of about 0.1 T. The maximum flux step for a single motor step of the middle ring corresponds to 0.18 mT. By using rotations of both rings, the flux can be adjusted to a precision better than 0.15 mT over the entire flux range. This minimum step size is not inherent in our design. It can easily be adjusted by changing the gear transmission ratio. In the present realization (gear ratios are ca. 1/5 and 1/4 for the middle and outer rings) the precision is sufficient for any standard pulsed EPR experiment, as the excitation bandwidth of the pulses is much larger.

3.3.2. Homogeneity of the magnetic field

The spatial dependence of the magnetic flux (B_z) within the probe bore of the magnet was measured with a 3D scanning Hall probe. Fig. 3 shows the average field and its standard deviation versus DSV. From this 3D measurement it was interpolated that the flux varies by about 0.3 mT (ca. 1000 ppm or 10^{-3}) over the volume of a standard EPR tube (3 mm inner diameter and 100 mm height) when positioned in the center of the bore. These values compare to a field homogeneity of about 5×10^{-6} for the much larger electromagnet of a commercial spectrometer. Clearly, the permanent magnet system is not suitable for all the applications of this commercial machine. However, the field inhomogeneity of 10^{-3} corresponds to a variation of the electron spin resonance frequency by about 8 MHz over the sample volume which compares to an excitation bandwidth of about 30 MHz in typical pulsed EPR experiments. Together with other contributions to inhomogeneous line broadening, such as g anisotropy and anisotropic hyperfine couplings, and unresolved isotropic hyperfine couplings, the line broadening due to magnetic field inhomogeneity is refocused in echo-detected EPR experiments. It is thus not expected to significantly influence the performance of echo-detected EPR experiments for the measurement of relaxation times, nuclear frequencies, or dipole–dipole couplings between electron spins. In field-swept echo-detected EPR and CW EPR experiments in the solid state the field inhomogeneity may cause significant line broadening for samples with particularly narrow lines, such as defect centers in crystals, exchange narrowed radicals or perdeuterated radicals and transition metal complexes. Unresolved proton hyperfine coupling in the solid state causes stronger broadening of the lineshape singularities than field inhomogeneity of this magnet for a majority of samples.

For CW EPR and field-swept echo-detected EPR in solution the achieved field homogeneity is not sufficient. In its current form the magnet may also not be suitable for the acquisition of high-quality line shapes of nitroxides in the solid state, as they are required to obtain information on short label-to-label distances by line shape analysis [21], unless sample volume is limited and narrower tubes are used. The field homogeneity could be improved by shim coils or magnets [22] without significantly compromising the low power consumption of the system.

However, recent improvements in magnet design and construction procedure lead to magnets which are at least one order of magnitude more homogeneous [14]. These improvements are due to the use of magnets with a polygonal footprint, optimized sorting algorithms, spacing of the rings along the x-axis and slight deviations from a perfectly circular arrangement of the magnets in a single ring [14].

3.4. Application in pulse EPR experiments

Although the prototype magnet was designed for a home-built S-band EPR spectrometer operating at a frequency of about

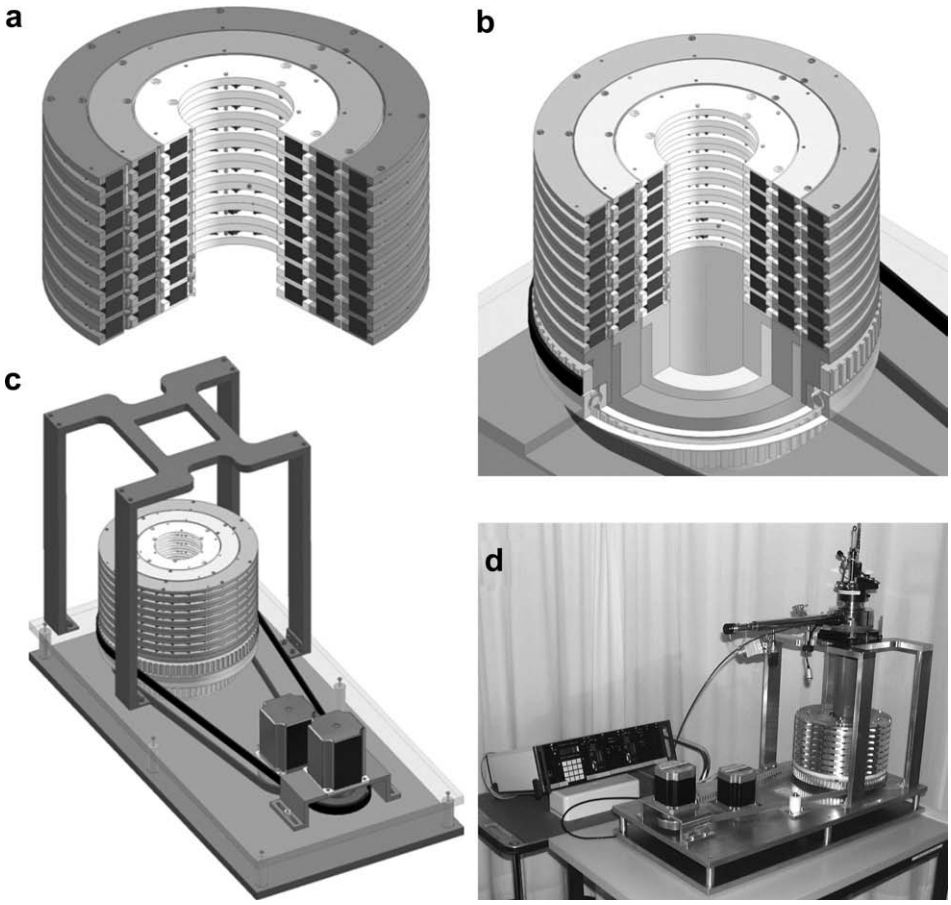

Fig. 2. Technical drawings and photograph of the magnet: (a) 8 layers from Fig. 1 are stacked to form the complete magnet (one quarter removed for better inspection). (b) Same as a) but also showing the ball bearings and belt drive which allows rotation of the two outer rings. (c) Complete assembled magnet system with stepper motors in the front and a support to rest probeheads and cryostats on. (d) Photograph of the prototype including a probehead inside a cryostat and the electronic control unit (left).

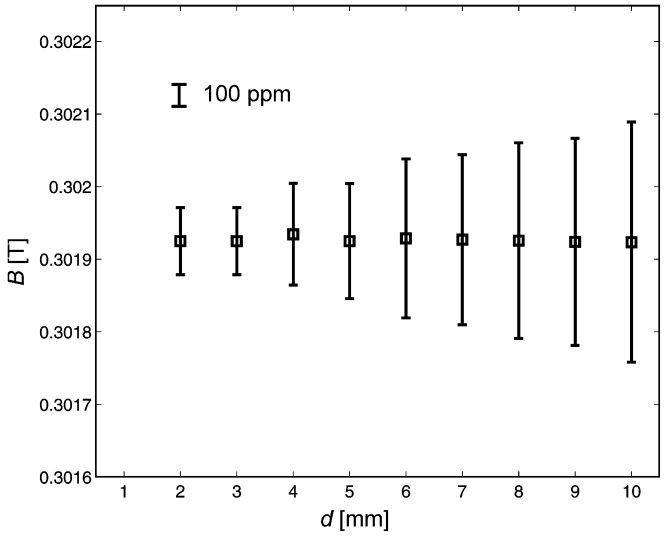

Fig. 3. Average and standard deviation of the magnetic flux B_0 over a spherical volume of diameter (DSV), d, in the center of the permanent magnet. Measured with a scanning Hall probe at max. flux and an ambient temperature of 23 ± 0.5 °C.

3.5 GHz, the upper end of the flux range at about 0.3 T also allows for experiments a X-band frequencies of about 9.75 GHz for special samples. To test resolution of nuclear frequencies and long-time stability of the magnet we could thus employ a commercial X-band EPR/ENDOR spectrometer and probe head. The sample is a single crystal of copper-doped glycine with a maximum electron spin g value of $g_{||} = 2.2644$. For the magnetic field near the normal of the square planar complex ($g_{||}$ orientation) the low-field line ($m_I(^{63,65}\mathrm{Cu}) = 3/2$) of the resolved hyperfine quartet of copper falls within the field range of our magnet. The single crystal was oriented so that such orientations could be accessed by turning the sample tube. Reference measurements in a similar orientation were performed with the electromagnet of the Bruker spectrometer.

To test the magnetic field sweep obtained by rotating the outer ring, a CW EPR spectrum of the $m_I(^{63,65}\mathrm{Cu}) = 3/2$ line was acquired (Fig. 4). The linewidth of 2.05 mT is due to only weakly resolved hyperfine coupling to the ^{14}N nuclei of the two glycine ligands. This hyperfine coupling of approximately 0.63 mT appears to be resolved. Published ENDOR data [23] suggest splittings between 0.55 and 0.65 mT at this orientation. The weak satellite line at low field (asterisk in Fig. 4) is also seen with the electromagnet (data not shown) and is thus not due to an imperfection of the magnet but due to an imperfection of the crystal.

The Mims ENDOR spectrum (Fig. 5) acquired at the field corresponding to maximum intensity of the $m_I(^{63,65}\mathrm{Cu}) = 3/2$ line demonstrates that magnetic field inhomogeneity does not pose a limitation on typical nuclear frequency spectra in the solid state. The peak-to-peak linewidth for the proton line at 9.28 MHz after pseudomodulation of the spectrum shown in Fig. 5 is 75 kHz, the same as for the corresponding line in a measurement with the electromagnet (data not shown). This is not surprising, as the field inhomogeneity of 10^{-3} corresponds to a variation in the ^{1}H Zeeman frequency of only 12.5 kHz. The linewidth of 75 kHz in a mea-

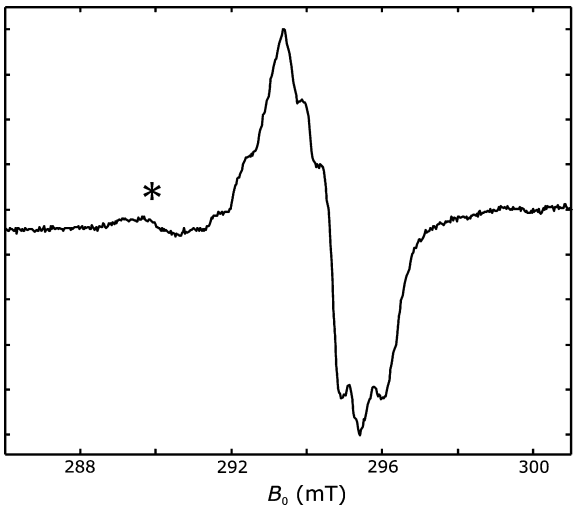

Fig. 4. CW EPR spectrum of the $m_I(^{63,65}\mathrm{Cu}) = 3/2$ line in a glycine single crystal doped with 1% copper nitrate taken at a temperature of 15 K. The crystal is oriented so that the magnetic field is nearly parallel to the coordination plane normal of the square planar complex. The asterisk denotes a satellite line due to an imperfection of the crystal.

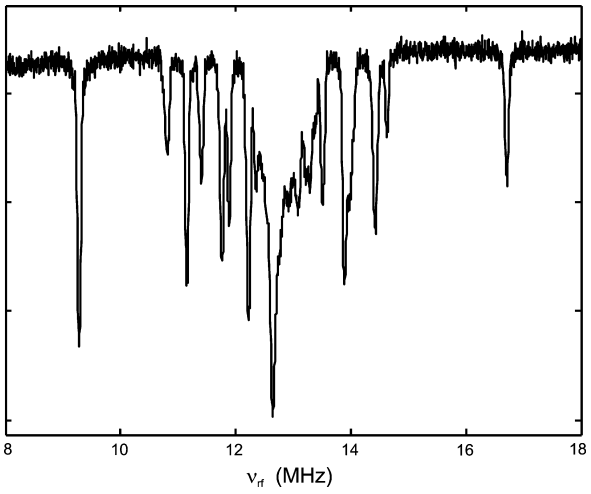

Fig. 5. Mims ENDOR spectrum taken at the maximum of the $m_I(^{63,65}\mathrm{Cu}) = 3/2$ line in a glycine single crystal doped with 1% copper nitrate. The measurement temperature was 15 K.

surement that extended over 1 h indicates that the magnetic field is stable in the regime where it is fixed. This stability is also confirmed in a time-domain pulsed EPR experiment that extended over about 30 min. The decay of the modulation in the three-pulse ESEEM data of the copper-doped glycine single crystal (Fig. 6) again corresponds to a linewidth of slightly less than 100 kHz as it is expected for ligand protons due to proton dipole–dipole coupling and paramagnetic relaxation in a solid. The decay rate of the unmodulated contribution to the stimulated echo is governed by spectral diffusion and is the same as in a control measurement performed with the electromagnet of the commercial spectrometer (data not shown).

4. Conclusion

The described magnet system was designed and constructed as a feasibility study in order to learn if EPR experiments can be reliably conducted using permanent magnets and a mechanical field sweep.

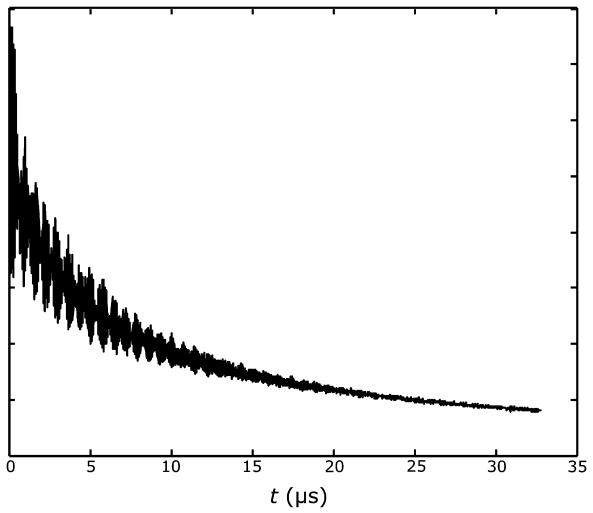

Fig. 6. Three-pulse ESEEM time trace taken at the maximum of the $m_I(^{63,65}\mathrm{Cu}) = 3/2$ line in a glycine single crystal doped with 1% copper nitrate.

Even without additional shim coils or magnets, the homogeneity of the magnet is sufficient for standard pulsed EPR experiments on solids. Linewidths of about 75 kHz were found in a Mims ENDOR spectrum of copper-doped glycine, the same as obtained with a commercial electromagnet. Nitrogen hyperfine splittings of about 0.6 mT were resolved in an X-band CW EPR spectrum of the same sample. In the latter case the spectrum was acquired while sweeping the magnetic field by rotation of the outer magnet ring with respect to the two inner ones. Although the current prototype magnet was designed for an S-band spectrometer and attains a maximum flux of 0.3 T, in the meantime we have learned to construct magnets for X-band operation with a maximum flux of 0.45 T and greatly improved homogeneity (ca. 10^{-5}) [14]. In this study we also learned that the use of 2 rings is sufficient for most applications because field positioning can be realized accurately enough using suitable gear ratios which greatly simplifies the construction.

In summary, we are convinced that a magnet design which merges the improved magnet from [14] with the mechanical sweep demonstrated here is well suited for solid-state EPR and will have a size and weight that will allow table top or (trans-)portable applications, provided that the console and microwave bridge can also be reduced in size.

Acknowledgment

The authors want to thank Prof. H.W. Spiess (Max-Planck Institute for Polymer Research, Mainz) for enabling this research in his lab and permitting access to the workshop.

References

[1] A. Schweiger, G. Jeschke, Principles of pulse electron paramagnetic resonance, 2001.
[2] A.D. Milov, A.G. Maryasov, Y.D. Tsvetkov, Pulsed electron double resonance (PELDOR) and its applications in free-radicals research, Appl. Magn. Reson. 15 (1998) 107–143.
[3] G. Jeschke, Distance measurements in the nanometer range by pulse EPR, Chem. Phys. Chem. 3 (2002) 927–932.
[4] G. Jeschke, Y. Polyhach, Distance measurements on spin-labelled biomacromolecules by pulsed electron paramagnetic resonance, Phys. Chem. Chem. Phys. 9 (2007) 1895–1910.
[5] O. Schiemann, T.F. Prisner, Long-range distance determinations in biomacromolecules by EPR spectroscopy, Quater. Rev. Biophys. 40 (2007) 1–53.
[6] M. Ikeya, M. Furusawa, A portable spectrometer for ESR microscopy, dosimetry and dating, Appl. Radiat. Isot. 40 (1989) 845–850.

[7] L.W. Rupp, K.R. Wittig, W.M. Wash, Miniature magnet for electron spin resonance experiments, Am. J. Phys. 44 (1976) 655–657.
[8] J.G. Shanks, F.-D. Tsay, W.K. Rhim, Miniature magnet assembly for NMR-ESR spectroscopy, Am. J. Phys. 48 (1980) 620–622.
[9] H. Ishii, M. Ikeya, An electron spin resonance system for in-vivo human tooth dosimetry, Jap. J. Appl. Phys. 29 (1990) 871–875.
[10] T. Kojima, Y. Haruyama, H. Tachibana, R. Tanaka, J. Okamoto, H. Hara, Y. Yamamoto, Development of portable ESR spectrometer as a reader for alanine dosimeters, Appl. Radiat. Isot. 44 (1993) 361–365.
[11] A. Nakanishi, N. Sugahara, A. Furuse, Portable ESR spectrometer with Neomax (Nd–Fe–B) permanent magnet circuit, Appl. Radiat. Isot. 44 (1993) 357–360.
[12] G. Moresi, R. Magin, Miniature permanent magnet for table-top NMR, Magn. Res. Engin. 19B (2003) 35–43.
[13] H. Raich, P. Blümler, Design and construction of a dipolar Halbach array with an homogeneous field from N * 8 Identical Bar-Magnets—NMR-Mandhalas-, Magn. Res. Engin. 23B (2004) 16–25.
[14] B.D. Armstrong, M.D. Lingwood, E.R. McCarney, E.R. Brown, P. Blümler, S. Han, Portable X-band system for solution state dynamic nuclear polarization, J. Magn. Reson. 191 (2008) 273–281.
[15] J.C. Mallinson, One-sided fluxes—a magnetic curiosity?, IEEE Trans Magn. 9 (1973) 678–682.
[16] K. Halbach, Strong rare earth cobalt quadropoles, IEEE Trans. Nucl. Sci. 26 (1979) 3882–3884.
[17] K. Halbach, Design of permanent multipole magnets with oriented rare earth cobalt material, Nucl. Inst. Meth. 169 (1980) 1–10.
[18] T.R. Ni Mhiocháin, J.M.D. Coey, D.L. Weaire, S.M. McMurry, Torque in nested Halbach cylinders, IEEE Trans. Magn. 35 (1999) 3968–3970.
[19] H.A. Leupold, E. Potenziani II, M.G. Abele, Applications of yokeless flux confinement, J. Appl. Phys. 64 (1988) 5994–5996.
[20] H.A. Leupold, Field adjustable transverse flux sources, US Patent, 1989.
[21] M.D. Rabenstein, Y.K. Shin, Determination of the distance between 2 spin labels attached to a macromolecule, Proc. Natl. Acad. Sci. USA 92 (1995) 8239–8243.
[22] E. Danieli, J. Mauler, J. Perlo, B. Blümich, Mobile sensor for high resolution NMR spectroscopy and imaging, J. Magn. Reson. 198 (2009) 80–87.
[23] M. Fujimoto, C.A. McDowell, T. Takui, Ligand ENDOR spectra of Cu(II) impurity complexes in a-glycine crystals, J. Chem. Phys. 70 (1979) 3694–3701.